Journal of The Electrochemical Society, **162** (3) A344-A349 (2015)
0013-4651/2015/162(3)/A344/6/$31.00 © The Electrochemical Society

Utilization of Al_2O_3 Atomic Layer Deposition for Li Ion Pathways in Solid State Li Batteries

Jae Ha Woo,[a] Jonathan J. Travis,[b] Steven M. George,[a,b] and Se-Hee Lee[a,*,z]

[a]*Department of Mechanical Engineering, University of Colorado at Boulder, Boulder, Colorado 80309-0427, USA*
[b]*Department of Chemistry and Biochemistry, University of Colorado at Boulder, Boulder, Colorado 80309-0215, USA*

Limited interfacial contact area between active material and solid state electrolyte (SSE) in solid state lithium batteries (SSLBs) can be addressed by utilizing a thermally treated Al_2O_3 atomic layer deposition (ALD) coating as a lithium ion transport pathway. SSLBs with a $LiCoO_2/Li_{3.15}Ge_{0.15}P_{0.85}S_4/77.5Li_2S$-$22.5P_2S_5/Li$ configuration were built and tested using charge-discharge cycles between $3.3 \sim 4.3$ V (vs. Li/Li^+) at a current density of 45 $\mu A\ cm^{-2}$. An increase of more than 10% in the inital discharge capacity as well as good cycling stability are achieved from SSLBs using $LiCoO_2$ particles coated with 2 and 4 cycles of Al_2O_3 ALD. The dQ/dV analysis, electrochemical impedance spectroscopy (EIS), and the overpotential study with galvanostatic intermittent titration technique (GITT) were conducted to elucidate the enhancement of Li^+ transport through Al_2O_3 ALD layers surrounding $LiCoO_2$.
 [DOI: 10.1149/2.0441503jes]

Manuscript submitted September 18, 2014; revised manuscript received October 28, 2014. Published December 23, 2014.

There are growing demands for sustainable and eco-friendly energy sources due to concerns over the impact of fossil fuels on the environment.[1] Li ion batteries (LIBs), which are widely used in many portable electronic devices, are one of the major candidates for energy storage systems in electric vehicles.[1,2] The development of a reliable LIB configuration to obtain stable cycling performance is necessary for LIBs to prevail against other non-fossil fuels. Organic liquid electrolytes are a common component in many LIBs which are used in many electronic devices and electric vehicles (EVs).[3,4] However, the ignitability of organic electrolytes used in conventional LIBs is one of the primary obstacles for large scale-up of LIB systems.[3,4] Solid state Li batteries (SSLBs), which use nonflammable solid state electrolytes (SSEs), are one of the promising solutions to the safety concerns over the flammability of the organic liquid electrolyte.[5]

Despite their improved safety performance, SSLBs have not been practical subsititutes for conventional LIBs because of their low power densities.[4] Previous works have shown that one of the major causes of relatively poor power performance of SSLBs can be attributed to the interfaces between active material and SSE in working electrodes.[4,6] SSLBs have less interfacial contact area from solid-solid contacts compared to the liquid-solid interfaces in coventional LIBs. The restricted pathways for Li^+ ions and electrons in SSLBs limit ionic and electronic transports which are essential for battery cycling. In addition, many previous works have shown with electrochemical impedance spectroscopy (EIS) and transmission electron microscopy (TEM) that the interfacial resistance at electrode/SSE interfaces ($LiCoO_2/80Li_2S \cdot 20P_2S_5$ SSE, $LiMn_2O_4/80Li_2S \cdot 20P_2S_5$ SSE) increases during charge-discharge processes.[6–10]

There have been many efforts to create better interfaces between active materials and SSEs in solid state batteries such as the employment of oxide coatings on active materials in working electrodes.[4,6–10] It is confirmed in these works that the resistance at the interface is greatly reduced by introduction of a passivating oxide layer. In addition, considerable increases in discharge capacities are observed from solid state batteries which use coatings of various oxide layers on active material pariticles in working electrodes compared to those which use uncoated active material pariticles.[4,6–10] The factors proposed for the role of the oxide layer in the enhancement are (i) the alleviation of resistive layer growth at the interface[6–8] and (ii) the possibility of an increase in the electrochemically active area at the interface.[7,10]

Although these reports about solid state batteries commonly state that the improvement of cycling performance comes from the decrease in the interfacial resistance at the active material/SSE interface, they don't necessarily focus on the way of utilizing oxide coatings to increase capacities of solid state batteries. To illuminate this issue, we focused on the role of the oxide coating not only in (i) but also in (ii) which are mentioned above. Previous works have shown that oxide coating layers on the surface of active materials used in organic liquid electrolyte batteries exhibit desirable properties after heat treatments (HTs).[11–13] Increases in capacities from the batteries using oxide coatings either on active materials or on working electrode also appear in these papers.[12,13] Nevertheless, they didn't clarify the effect of the oxide layers with/without HT either on the active materials or on the working electrodes of Li batteries.

On the other hand, our group demonstrated a novel way of introducing Al_2O_3 coating on the surface of $LiCoO_2$.[14–16] Utilization of atomic layer deposition (ALD) of Al_2O_3 onto the active material resulted in great improvements in cycling performances for both liquid electrolyte Li battery and SSLB. In addition, Jung et al. reported that HT of Al_2O_3 ALD layer on the electrode helped to create a beneficial layer for Li^+ ion transport in liquid electrolyte Li batteries.[17]

In this study, we present a breakthrough in overcoming limited interfaces in SSLBs by the utilization of Al_2O_3 ALD layer on $LiCoO_2$ in the working electrode using HT. SSLBs with the double layer SSE configuration used in our previous work[16] were constructed using $LiCoO_2$ powders coated with Al_2O_3 ALD which were heat treated in Ar environment after ALD process. Galvanostatic charge-discharge behaviors, differential capacity(dQ/dV) analysis, EIS profiles, and electrochemical overpotentials obtained from galvanostatic intermittent titration technique (GITT) were studied to determine the effect of HT on Al_2O_3 ALD layer surrounding $LiCoO_2$ particle. Results corroborate our statement of the beneficial Li^+ ion pathway formed from Al_2O_3 ALD layers.

Experimental

As-ball-milled (ABM) $Li_{3.15}Ge_{0.15}P_{0.85}S_4$ SSE and ABM $77.5Li_2S$–$22.5P_2S_5$ (mol%) SSE were synthesized by planetary ball milling (PBM) with the same method described in our previous work.[16] Heat treatment (HT) for ABM $Li_{3.15}Ge_{0.15}P_{0.85}S_4$ SSE powder was carried out inside the glove box on a hot plate with the heating rate of $+10°C\ min^{-1}$ to 460°C in a sealed glass container. SSE was kept at 460°C on the hot plate for 2 hours before being removed and placed on a cooling rack. All sample preparations and HTs were performed in a dry Ar-filled glove box.

Al_2O_3 ALD layers were coated directly on $LiCoO_2$ powders (LICO Technology Corp.) using a rotary reactor as mentioned in our former report.[14] $LiCoO_2$ powders with Al_2O_3 ALD layers were either put under a constant Ar gas flow using a sealed quartz tube in a furnace for HT (300°C, 12 hours) or dried using a vacuum oven (120°C, 12 hours). $LiCoO_2$ (uncoated/Al_2O_3 ALD-coated), heat-treated $Li_{3.15}Ge_{0.15}P_{0.85}S_4$ SSE, and acetylene black (AB, Alfa-Aesar, 50% compressed) were mixed at a weight ratio of 20:30:3 using a mortar and a pestle to prepare the working electrode composite for SSLBs. SSLBs with the double layer SSE configuration using Li

*Electrochemical Society Active Member.
[z]E-mail: sehee.lee@colorado.edu

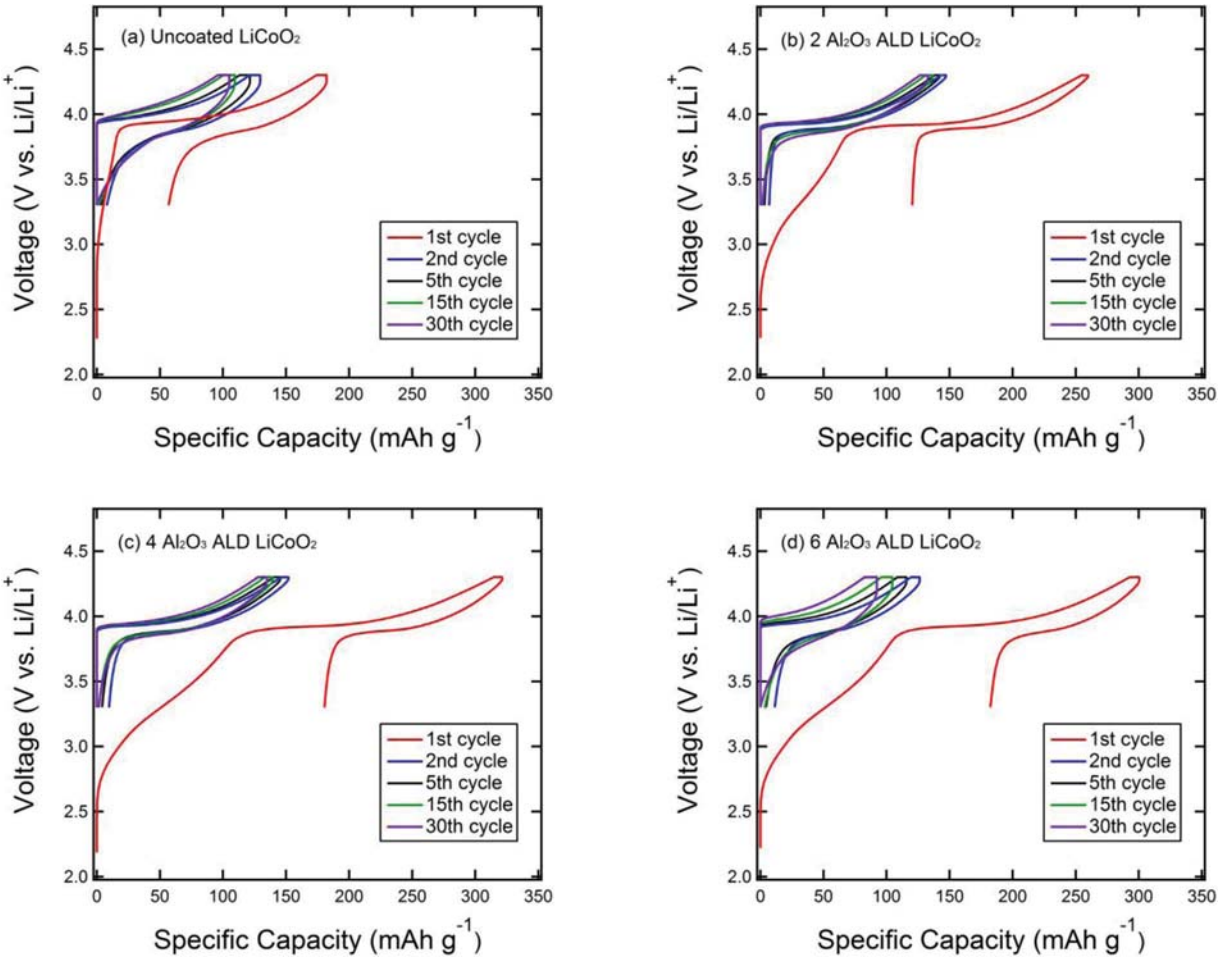

Figure 1. Voltage profiles of SSLBs using various Al_2O_3 ALD-coated $LiCoO_2$ particles.

metal foils as counter electrodes were constructed as described in our previous work.[16] All SSLB fabrications and experimental operations were implemented in polyaryletheretherketone (PEEK) molds (φ = 1.3 cm) with Ti metal cylinders as current collectors for both working and counter electrodes.

Galvanostatic charge-discharge processes were performed with SSLBs between 3.3 ∼ 4.3 V (vs. Li/Li^+) at a current of 45 $\mu A\ cm^{-2}$ at 30°C using an Arbin BT2000. Charge process and discharge process correspond to the delithiation and the lithiation of $LiCoO_2$. SSLBs were charged to 4.3 V (vs. Li/Li^+) and held at the voltage for 1 hour before discharge processes. All SSLB constructions and experiments were conducted in a dry Ar gas environment.

Electrochemical impedance spectroscopy (EIS) of SSLBs using $LiCoO_2$ particles with different surface conditions was performed by a Solartron 1280C. SSLBs were charged to 4.3 V (vs. Li/Li^+) with a current of 45 $\mu A\ cm^{-2}$ and held at the voltage for 1 hour before EIS measurements were made at the open-circuit voltage. AC impedance data were collected using an amplitude of 10 mV and a frequency range from 20 kHZ to 1 mHz.

A 2032-type coin cell was made for galvanostatic intermittent titration technique (GITT) measurement. A working electrode composite was prepared by spreading a slurry of $LiCoO_2$ powders (LICO Technology Corp.), acetylene black (AB, Alfa-Aesar, 50% compressed), and polyvinylidene fluoride(PVDF) (80:10:10 weight ratio) onto a high grade Al foil and roll-pressed after drying in air at 80°C for 1 hour. The electrodes were dried in a vacuum oven at 120°C for 12 hours before battery fabrication. The separator was a glass micro-fiber disk (Whatman GF/F) and the electrolyte was 1 M $LiPF_6$ in ethylene carbonate (EC): diethylene carbonate (DEC) (1:1 volume ratio). The cell fabrication was done in a dry Ar gas environment using Li metal as a counter electrode. The cell was charged and discharged between 3.3 ∼ 4.3 V (vs. Li/Li^+) by applying a constant C/10 rate current and 1 hour voltage hold at 4.3 V (vs. Li/Li^+) for the 1st cycle. For the 2nd cycle, a constant current density was applied (with the current density same as C/10 rate) followed by an open circuit stand of the cell for 3600 sec. This GITT procedure was performed at the 2nd charge-discharge process between 3.3 ∼ 4.3 V (vs. Li/Li^+).

Results and Discussion

Galvanostatic charge-discharge cycles were performed between 3.3 ∼ 4.3 V (vs. Li/Li^+) with SSLBs using $LiCoO_2$ particles coated with different numbers of Al_2O_3 ALD layers and with different HT environments. Figure 1 describes voltage profiles of SSLBs using various Al_2O_3 ALD-coated $LiCoO_2$ particles. All of Al_2O_3 ALD-coated $LiCoO_2$ particles used in this figure went through HT in Ar gas flow (300°C, 12 hours) before battery fabrication. What we can see from the figure are relatvely larger 1st charge capacities of SSLBs with Al_2O_3 ALD-coated $LiCoO_2$ particles compared to that of SSLB with uncoated $LiCoO_2$ particles. Since the only difference between them is the existence of Al_2O_3 ALD layer, we attribute additional charge capacities to interactions between the Al_2O_3 ALD layer and $Li_{3.15}Ge_{0.15}P_{0.85}S_4$ SSE which may result in enhanced Li^+ ion transport through the Al_2O_3 ALD layer. Further investigation is needed to clarify the mechanism of the reaction during the 1st charge process in our future work.

In addition, voltage profiles of subsequent cycles from SSLBs using $LiCoO_2$ particles coated with different numbers of Al_2O_3 ALD

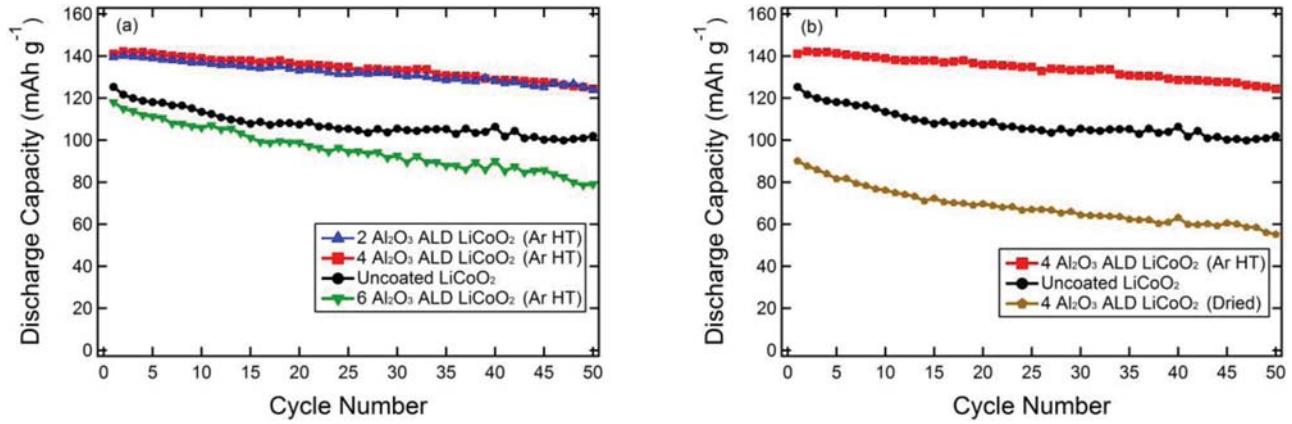

Figure 2. Cycling performances of SSLBs with (a) different numbers of Al_2O_3 ALD layers and (b) different HT environments.

layers are shown in Fig. 1. SSLB with uncoated $LiCoO_2$ reveals an increase in the polarization and a decrease in the specific capacity as the number of cycles increases (Fig. 1a). In contrast, SSLBs using $LiCoO_2$ particles with 2 & 4 Al_2O_3 ALD layers shows less polarization and less degradation in the specific capacity during cycling (Fig. 1b & 1c). We attribute this phenomenon to the suppresion of the resistive interfacial layer growth at $LiCoO_2$/SSE interface by Al_2O_3 ALD layer which was also observed in our previous work.[16] However, SSLB using $LiCoO_2$ particles with 6 Al_2O_3 ALD layers exhibits worse cycling performance even compared with SSLB using uncoated $LiCoO_2$ particles (Fig. 1d). The electronically insulating properties of thick Al_2O_3 ALD layers is thought to be the cause.[14,18] Authors speculate that the HT method used in this work is insufficient to address the insulating characteristics of Al_2O_3 layers from 6 cycles of ALD.

Galvanostatic cycling performances of different SSLBs between 3.3 ~ 4.3 V (vs. Li/Li^+) are compared in Figure 2. $LiCoO_2$ particles coated with Al_2O_3 ALD layers used in Fig. 2a were heat-treated in Ar gas flow (300°C, 12 hours) prior to battery fabrication. SSLBs using $LiCoO_2$ particles with 2 & 4 Al_2O_3 ALD layers show larger initial discharge capacities (~140 mAh g^{-1}) than that of SSLB using uncoated $LiCoO_2$ particles (125 mAh g^{-1}). This is more than a 10% increase in capacity which brings the capacity closer to the theoretical capacity of $LiCoO_2$.[8] Authors attribute this to the participation of Al_2O_3 ALD layers on Li^+ ion transport to $LiCoO_2$ which results in an increase of discharge capacities. On the other hand, SSLB with $LiCoO_2$ particles with 6 Al_2O_3 ALD layers exhibits worse cycling performance than that of SSLB using uncoated $LiCoO_2$ particles. The low discharge capacity and the inferior stability can be attributed to the insulating property of thick Al_2O_3 ALD layer as mentioned in Fig. 1d.

The effect of HT in Ar gas flow on the utilization of Al_2O_3 ALD layers on $LiCoO_2$ particles as Li^+ ion pathways is also studied (Fig. 2b). $LiCoO_2$ particles with 4 Al_2O_3 ALD layers were dried in a vacuum (120°C, 12 hours) and used for SSLB fabrication. The SSLB using dried ALD-coated $LiCoO_2$ particles achieved poor results compared to the SSLB using ALD-coated $LiCoO_2$ particles after HT under Ar gas flow (300°C, 12 hours). This is evidence showing that HT under Ar environment is integral for improvement of Li^+ ion transport in Al_2O_3 ALD layers surrounding $LiCoO_2$. It is believed that ionic diffusion occurs between $LiCoO_2$ and Al_2O_3 ALD layer during the HT process. Oh et al. showed that such ionic diffusion enhances electronic conductivity of Al_2O_3 layer on $LiCoO_2$.[13] More detailed analysis of the change in properties of Al_2O_3 ALD layer after HT will be done in future studies.

In order to understand electrochemical reactions occurred on $LiCoO_2$ particles with various surface conditions, dQ/dV values were calculated (Fig. 3) from charge-discharge profiles of SSLBs in Fig. 2b. All 3 SSLBs using different $LiCoO_2$ particles in working electrodes exhibit major redox peaks which correspond to Li^+ intercalation/deintercalation with $LiCoO_2$ at ~3.9 V (vs. Li/Li^+).[19] However, significant difference exists in these dQ/dV profiles. Noticeable humps appear at ~3.3 V (vs. Li/Li^+) in dQ/dV plots from SSLBs using Al_2O_3 ALD-coated $LiCoO_2$ particles (Ar HT, dried). These humps are expected to correspond to the interaction between Al_2O_3 ALD layer and $Li_{3.15}Ge_{0.15}P_{0.85}S_4$ SSE which is mentioned in Fig. 1. It seems that additional oxide layers added at $LiCoO_2$/SSE interfaces interact with surroundings to result in higher charge capacities in the 1st charge process. As a result of this interaction, Al_2O_3 ALD-coated $LiCoO_2$ with Ar HT shows sharper and larger major peaks at ~3.9 V (vs. Li/Li^+) which can be explained as more effective access to Li^+ ion reaction sites on $LiCoO_2$ particles during charge-discharge cycling, achieving larger capacities. On the contrary, dried Al_2O_3 ALD-coated $LiCoO_2$ exhibits blunt and smaller major peaks at ~3.9 V (vs. Li/Li^+) which result in low capacities as shown in Fig. 2b. Therefore Ar HT process seems to be integral to enhance transport properties of Al_2O_3 ALD layer on $LiCoO_2$.

AC impedance spectroscopic analyses of the SSLBs with different active materials (Ar HT 4 Al_2O_3 ALD $LiCoO_2$, uncoated $LiCoO_2$, and dried 4 Al_2O_3 ALD $LiCoO_2$) are presented in Fig. 4. EIS data were collected after the 1st charge process to focus on the interfacial resistance of $LiCoO_2$/SSE interface at initial stage and to exclude the increase in the resistance at $LiCoO_2$/SSE interface during cycling which was shown in our previous report.[16] All profiles show semicircles which correspond to charge transfer resistance at the interface between $LiCoO_2$ and $Li_{3.15}Ge_{0.15}P_{0.85}S_4$ SSE.[8] The SSLB with Ar HT 4 Al_2O_3 ALD $LiCoO_2$ (Fig. 4a) shows smaller interfacial resistance compared to the SSLB with dried 4 Al_2O_3 ALD $LiCoO_2$ (Fig. 4c). It can be attributed to an enhancement in charge transfer in Al_2O_3 ALD layer after Ar HT which contributes to better cycling performance as shown in Fig. 2b. However, it should be noted that Ar HT 4 Al_2O_3 ALD $LiCoO_2$ (Fig. 4a) does not show improvement in charge transfer resistance compared to uncoated $LiCoO_2$ (Fig. 4b). Based on EIS analysis, it is believed that superior performance of the SSLB using Ar HT 4 Al_2O_3 ALD $LiCoO_2$ compared to the SSLB using uncoated $LiCoO_2$ is related to the mass transfer of Li^+ ion rather than the charge transfer at the interface.

Along with EIS study, elucidation for the transport properties of $LiCoO_2$ particles with various surface conditions is performed by comparing overpotentials from SSLBs using them. It has been shown that the overpotential of an electrochemical cell can be a way of investigating the transport properties of an active material in a cell.[20] Figure 5 assesses varying overpotentials of different SSLBs by comparing each voltage profile to the thermodynamic equilibrium voltage points of a $LiCoO_2$/Li half cell. Voltage profiles from the 2nd cycles are selected for SSLBs to exclude the effect of the 1st charge reaction which accompanied interaction at Al_2O_3 ALD layer/$Li_{3.15}Ge_{0.15}P_{0.85}S_4$ SSE interface and to minimize the effect of degradation during cycles. Equilibrium points were obtained by

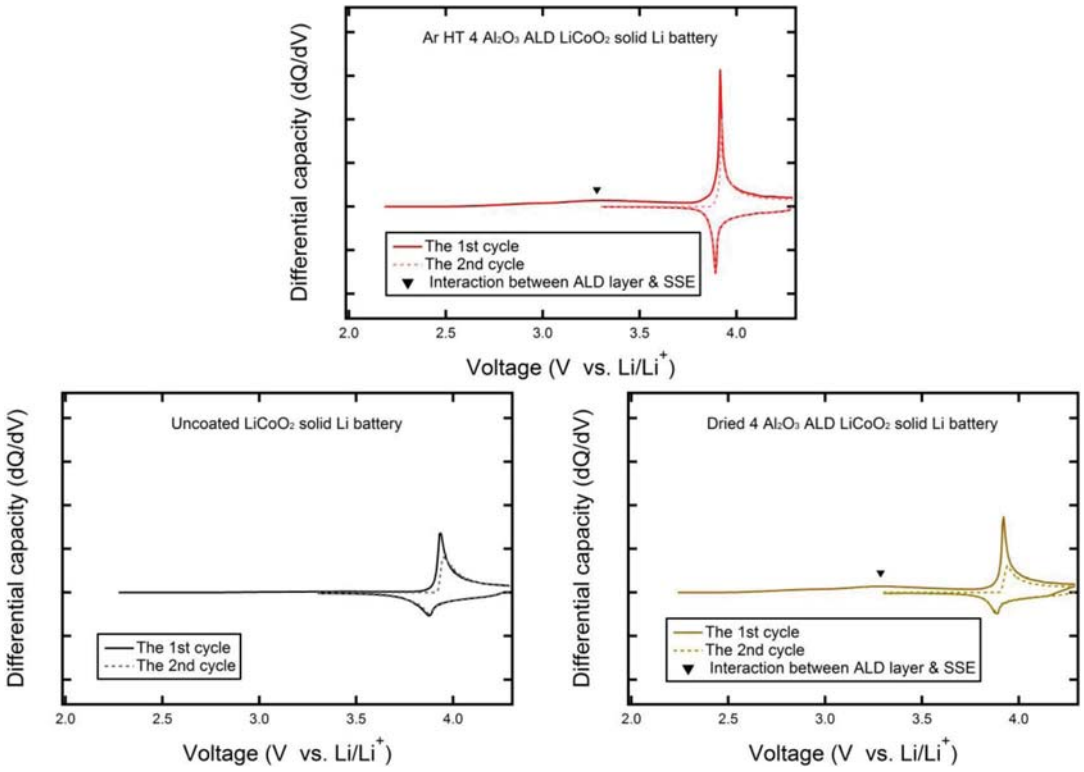

Figure 3. dQ/dV profiles of SSLBs with different $LiCoO_2$ particles.

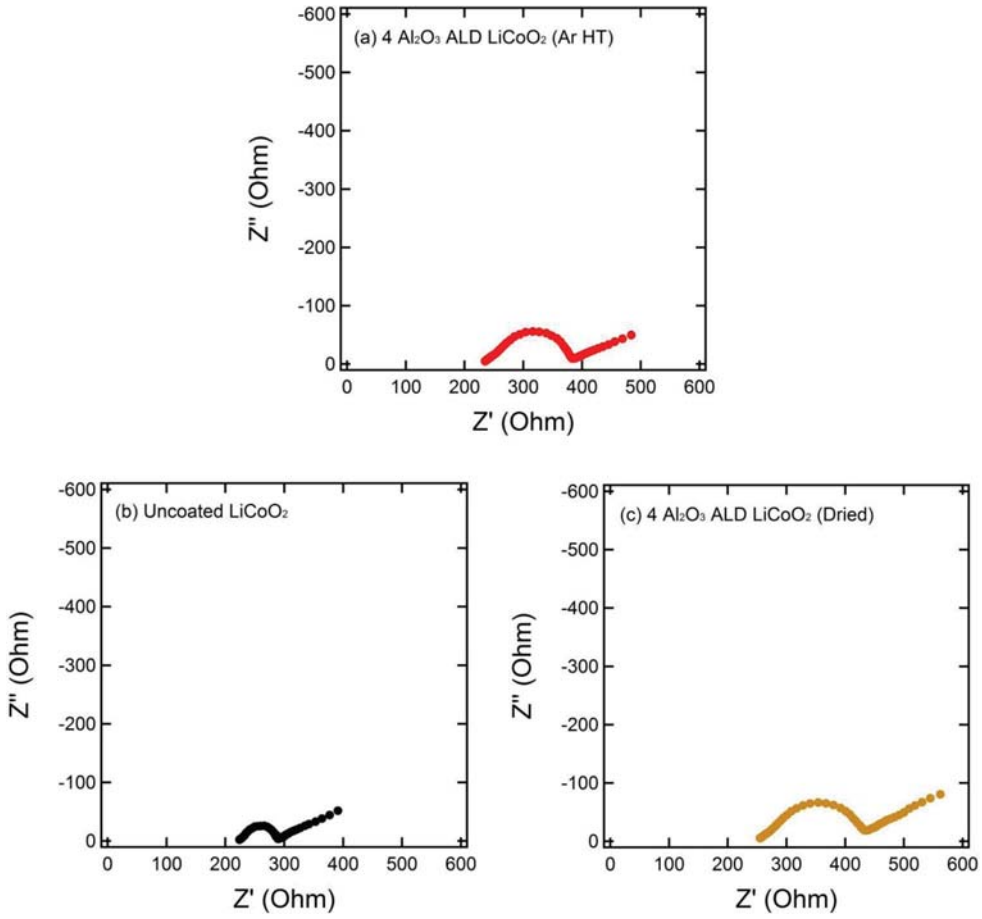

Figure 4. AC impedance profiles of SSLBs using $LiCoO_2$ with different surface conditions after the 1st charge process.

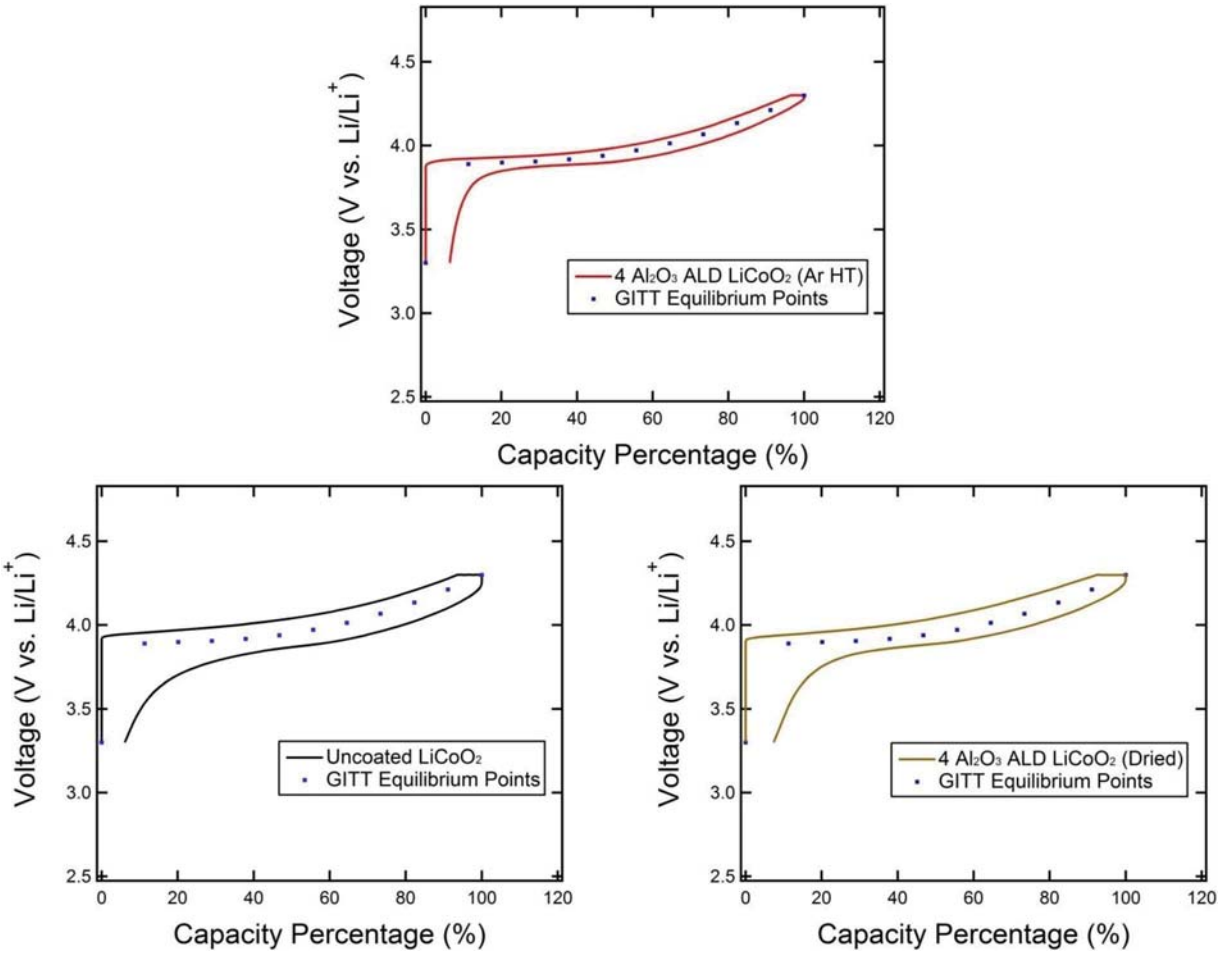

Figure 5. Comparison between GITT equilibrium voltage points and 2nd charge-discharge voltage profiles of SSLBs with different $LiCoO_2$ particles. Profiles are normalized to 100% of their charge capacities for the comparison.

applying galvanostatic intermittent titration technique (GITT) to $LiCoO_2$/Li 2032-type coin cell using liquid electrolyte. Average values between voltage points of the coin cell after each open circuit stand during the 2nd charge process and those during the 2nd discharge process are selected as equilibrium points. In addition, all profiles are normalized to 100% of their charge capacities for the comparison. It is obvious that 4 Al_2O_3 ALD $LiCoO_2$ after Ar HT shows the smallest overpotential compared to uncoated $LiCoO_2$ and dried 4 Al_2O_3 ALD $LiCoO_2$. Therefore, it can be concluded that Al_2O_3 ALD layers surrounding $LiCoO_2$ particles have better mass transport property after Ar HT. As a result, it can be expected to provide better Li^+ ion intercalation. On the other hand, 4 Al_2O_3 ALD $LiCoO_2$ without HT showed a large overpotential comparable to the uncoated one. According to EIS analysis and the overpotential study, the relatively poor transport properties of the non-HT ALD layer for both mass and charge transfer resulted in the worst cycling performance in Fig. 2b.

Based on experimental results shown above, we propose a mechanism of the utilization of Al_2O_3 ALD layer for efficient access to Li^+ ion reaction sites on $LiCoO_2$. It has been widely accepted that reversible Li^+ ion intercalation into $LiCoO_2$ occurs through two-dimensional pathways.[21–23] $LiCoO_2$ has the rhombohedral (space group $R\bar{3}m$) layered structure composed of alternating CoO_2 sheets and sheets of octahedrally coordinated Li^+ ions. Li^+ ions intercalate and deintercalate through gaps between CoO_2 sheets. Therefore, the intercalation is dependent on the direction of Li^+ ion movement. We can expect that soaking $LiCoO_2$ particles with liquid electrolyte will provide sufficient Li^+ ion pathways within the working electrode.

However, limited interfacial contact area between active material and SSE in working electrodes of SSLBs makes matters worse. Figure 6a shows how the number of effective interfaces for Li^+ ion intercalation is limited in a SSLB's working electrode. The number of contacts between $LiCoO_2$ particles and SSE particles in a SSLB

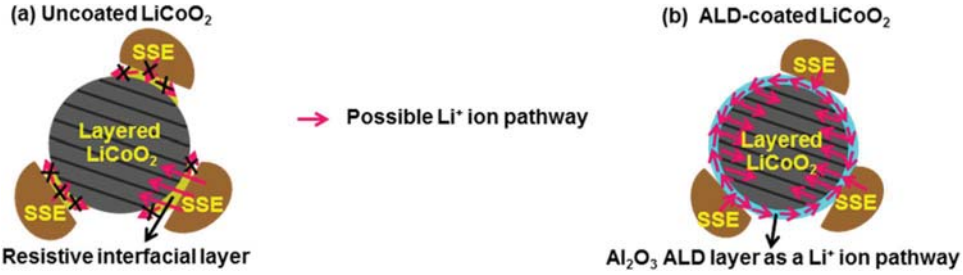

Figure 6. Schematic depiction of the interface between (a) uncoated $LiCoO_2$ & SSE, (b) Ar HT Al_2O_3 ALD-coated $LiCoO_2$ & SSE.

is less than that of a liquid electrolyte battery. Among those limited contacts, effective Li^+ ion intercalation only occurs when the Li^+ ion movement direction is along the gap between CoO_2 sheets in a $LiCoO_2$ particle. In addition, a resistive interfacial layer which hinders Li^+ ion transport can develop during cycling of SSLBs.[16] Therefore, we believe that these factors stated above are the reasons for lower capacities and faster degradation of SSLBs compared to those of liquid electrolyte Li batteries.

Figure 6b depicts our proposed mechanism of the utilization of Al_2O_3 ALD layer. HT of the Al_2O_3 ALD layer in Ar gas flow allows the ALD layer to serve as a Li^+ ion pathway providing additional access to intercalation sites for Li^+ ions in $LiCoO_2$. This will result in an increase in battery capacity which is needed for higher energy density. In addition, the Al_2O_3 ALD layer can help to suppress the growth of resistive interfacial layers between $LiCoO_2$ and SSE particles[16] during battery cycling. As a result, $LiCoO_2$ with Ar HT Al_2O_3 ALD layer can achieve high energy density and long-term cycling stability which are essential for the application of Li ion batteries in EV applications.

Conclusions

Heat treatment in Ar gas flow of Al_2O_3 ALD coated $LiCoO_2$ particles is utilized as a method to improve Li^+ ion transport on the surface of particles. Larger 1st charge capacities are observed from SSLBs with Al_2O_3 ALD-coated $LiCoO_2$ compared to SSLBs with uncoated ones due to the interaction between the heat treated ALD layer and SSE. $LiCoO_2$ particles coated with 2 & 4 cycles of Al_2O_3 ALD and subsequently HT under Ar gas flow achieve smaller polarization increases, relatively larger initial discharge capacities, and better cycling performances compared to those from SSLBs with uncoated $LiCoO_2$ particles. However, $LiCoO_2$ particles coated with 6 cycles of Al_2O_3 ALD and subsequently HT under Ar gas flow show worse performance due to the insulating property of the thicker Al_2O_3 ALD layer. Also, it is shown that HT in Ar gas flow is essential for improving the Al_2O_3 ALD layer's effect on SSLB performance by comparing 4 Al_2O_3 ALD layers with and without HT. Al_2O_3 ALD layer on $LiCoO_2$ seems to exhibit more efficient Li^+ ion transport after HT according to dQ/dV analysis, EIS studies, and the overpotential study with GITT method. We demonstrate that Al_2O_3 ALD layer coated on $LiCoO_2$ can be utilized as an additional Li^+ ion transport pathway. Therefore, this work proposes an effective strategy to overcome the limited interface issue in SSLBs. More sophisticated studies on the mechanism of the interaction between $LiCoO_2$, Al_2O_3 ALD layer, and SSE during HT & the 1st charge will be performed in future works.

Acknowledgments

This work was supported by the National Science Foundation (NSF, CHE-1231048). J.J.T. is grateful for the support from the Department of Energy through the DOE-BATT program.

References

1. M. Armand and J.-M. Tarascon, *Nature*, **451**, 652 (2008).
2. J.-M. Tarascon and M. Armand, *Nature*, **414**, 359 (2001).
3. F. Mizuno, A. Hayashi, K. Tadanaga, T. Minami, and M. Tatsumisago, *J. Power Sources*, **124**, 170 (2003).
4. N. Ohta, K. Takada, L. Zhang, R. Ma, M. Osada, and T. Sasaki, *Adv. Mater.*, **18**, 2226 (2006).
5. J. W. Fergus, *J. Power Sources*, **195**, 4554 (2010).
6. A. Sakuda, A. Hayashi, and M. Tatsumisago, *Chem. Mater.*, **22**, 949 (2010).
7. A. Sakuda, H. Kitaura, A. Hayashi, K. Tadanaga, and M. Tatsumisago, *J. Electrochem. Soc.*, **156**, A27 (2009).
8. A. Sakuda, H. Kitaura, A. Hayashi, K. Tadanaga, and M. Tatsumisago, *J. Power Sources*, **189**, 527 (2009).
9. A. Sakuda, A. Hayashi, and M. Tatsumisago, *J. Power Sources*, **195**, 599 (2010).
10. H. Kitaura, A. Hayashi, K. Tadanaga, and M. Tatsumisago, *Solid State Ionics*, **192**, 304 (2011).
11. Y. J. Kim, T.-J. Kim, J. W. Shin, B. Park, and J. Cho, *J. Electrochem. Soc.*, **149**, A1337 (2002).
12. Y. J. Kim, H. Kim, B. Kim, D. Ahn, J.-G. Lee, T.-J. Kim, D. Son, J. Cho, Y.-W. Kim, and B. Park, *Chem. Mater.*, **15**, 1505 (2003).
13. S. Oh, J. K. Lee, D. Byun, W. I. Cho, and B. W. Cho, *J. Power Sources*, **132**, 249 (2004).
14. Y. S. Jung, A. S. Cavanagh, A. C. Dillon, M. D. Groner, S. M. George, and S.-H. Lee, *J. Electrochem. Soc.*, **157**, A75 (2010).
15. I. D. Scott, Y. S. Jung, A. S. Cavanagh,Y. Yan, A. C. Dillon, S. M. George, and S.-H. Lee, *Nano Lett.*, **11**, 414 (2011).
16. J. H. Woo, J. E. Trevey, A. S. Cavanagh, Y. S. Choi, S. C. Kim, S. M. George, K. H. Oh, and S.-H. Lee, *J. Electrochem. Soc.*, **159**, A1120 (2012).
17. Y. S. Jung, A. S. Cavanagh, Y. Yan, S. M. George, and A. Manthiram, *J. Electrochem. Soc.*, **158**, A1298 (2011).
18. M. D. Groner, J. W. Elam, F. H. Fabreguette, and S. M. George, *Thin Solid Films*, **413**, 186 (2002).
19. J. N. Reimers and J. R. Dahn, *J. Electrochem. Soc.*, **139**, 2091 (1992).
20. J. Sun, K. Tang, X. Yu, J. Hu, H. Li, and X. Huang *Solid State Ionics*, **179**, 2390 (2008).
21. K. Mizushima, P. C. Jones, P. J. Wiseman, and J. B. Goodenough, *Mat. Res. Bull.*, **15**, 783 (1980).
22. G. G. Amatucci, J. M. Tarascon, and L. C. Klein, *J. Electrochem. Soc.*, **143**, 1114 (1996).
23. P. J. Bouwman, B. A. Boukamp, H. J. M. Bouwmeester, and P. H. L. Notten, *Solid State Ionics*, **152–153**, 181 (2002).